Journal Pre-proof

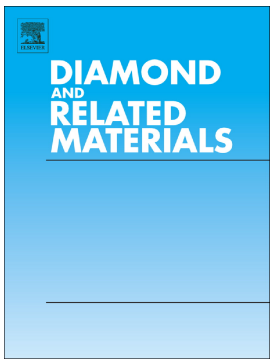

Carbon nanoparticles production using solvent assisted hydrothermal carbonization

Diego Flores Oña, Andrés Fullana

PII: S0925-9635(20)30513-6

DOI: https://doi.org/10.1016/j.diamond.2020.107960

Reference: DIAMAT 107960

To appear in: *Diamond & Related Materials*

Received date: 14 March 2020

Revised date: 12 May 2020

Accepted date: 27 May 2020

Please cite this article as: D.F. Oña and A. Fullana, Carbon nanoparticles production using solvent assisted hydrothermal carbonization, *Diamond & Related Materials* (2020), https://doi.org/10.1016/j.diamond.2020.107960

CARBON NANOPARTICLES PRODUCTION USING SOLVENT ASSISTED HYDROTHERMAL CARBONIZATION

Diego Flores Oña[1*], Andrés Fullana [2]

[1]*Affiliation1: Chemical Engineering Faculty, Universidad Central del Ecuador, Quito, Ecuador*

[2]*Affiliation2: Department of Chemical Engineering, Universidad de Alicante, Alicante, Spain*

Abstract

In this study, carbon nanoparticles (CNP) have been synthetized by the method of hydrothermal carbonization (HTC), which entails low cost, minimum equipment requirement, and less synthesis time. In order to improve the characteristics and the mass yield of CNP, a variation in the HTC process has been developed; which consists in introducing a blend of organic solvent with water into the reactor, instead of only water. The precursor is the glucose and three organic solvents were tested: hexane, toluene, and butyl acetate at different reaction times: 1, 2 and 4 hours. The size distribution of the CNP doesn't depend on the synthesis conditions. But, the mass yields of the CNP has an incredibly increase with the variation of process, this phenomenon is observed with all organic solvents at only one hour of reaction time. With butyl acetate the highest degree of dehydration was achieved according to the Ven Krevelen diagram and the FT-IR spectra. Besides, with this organic solvent, the highest Photoluminescence Quantum Yield was reached.

Keywords: Hydrothermal Carbonization; Carbon Nanoparticles; Solvent Extraction; Glucose.

1. Introduction

In the last decades, new carbonaceous materials have appeared, they stand out for the excellent physicochemical properties that make them ideal for applications; such as, bioimage [1], solar cells [2], ion sensors [3], controlled release of drugs [4], adsorption [5], supercapacitors [6], and photocatalysis [7]. These new materials are the Carbon Nanoparticles (CNP) that can have a spherical, ellipsoidal or, tubular shape; and within this group are fullerene, graphene, graphene

*Corresponding author. Tel: +593-996606480
e-mail: drflores@uce.edu.ec (Diego Flores)

oxide, nanotubes, nanowires, nanofibers, nanodiamonds, nanospheres, hybrid materials and Carbon Quantum Dots (CQDs).

CNP are remarkably important because their synthesis is relatively easy and cost-effective [8-10]. They are photobleaching resistant [11] and easily water dispersed [12]. They have a chemical surface that can be functionalized. With this, CNP acquire chemical stability, biocompatibility [13] and characteristics to be used in some medical applications [14]; for example, nuclear targeting cells [15,16]. Moreover, they have luminescent properties equal to or better than semiconductor nanomaterials based on metals such as cadmium, selenium, tellurium or lead, which makes them a promising material for photocatalysis [17].

There are two approaches for CNP production: top-down and bottom-up. The first one carries out the synthesis from carbon structures that have already been formed. Whilst, the second one uses simple molecules as precursors to form the nanoparticles by a polymerization process. Among the top-down methods are: laser ablasion [18], chemical oxidation of arc-discharge [19], electrochemical oxidation [20], and many more. The bottom-up methods are: pyrolysis [21], assisted processes with microwaves [22] and hydrothermal carbonization (HTC).

HTC is one of the most used methods for the synthesis of these nanomaterials, because it performs the process in mild conditions. In addition, it does not require expensive equipment or reagents. In fact, raw materials are abundant, and they do not require pre-treatment to eliminate moisture. HTC process allows us to functionalize the CNP surface [23]. In the regular HTC process, an aqueous solution with a precursor as a carbon source is introduced in a closed reactor. Afterwards, it is brought to a selected temperature and time. The pressure in the reactor is self-generated and the temperatures are in the range of 170 ^{o}C to 350 ^{o}C. Three products are generated: a solid carbonaceous material known as hydrochar; a liquid containing soluble substances; such as, furans, organic acids, aldehydes; and the third product is the CNP which are dispersed in water. A gaseous current is also produced, which is composed of gases including; CO_2, CO, CH_4 and H_2.

The first HTC study to obtain carbonaceous materials was made at the beginning of the 20th century using saccharides as raw material sources. Since then, a lot of research has been carried out with different carbon sources, ranging from simple molecules; such, as glucose, fructose or sucrose [24], to complex molecules like, starch [25], cellulose [26] and different types of

biodegradable biomass of vegetable, animal or industrial origin; for instance, orange juice [27], banana juice [28], milk [29], human hair [30], among others. Inside the reactor many reactions may occur: hydrolysis, dehydration, decarboxylation, and condensation, which can be consecutive or parallel [31]. The principal product of the reaction is 5-(hydroxymethyl) furfural [32,33] (HMF) together with other furans in smaller proportion. These components create the hydrochar and the CNP by means of aromatization and polymerization processes [34]. Due to the reaction conditions of the process, temperature gradients are formed [35], which together with the HMF, furans and gases; produce environments in which characteristics of the final product are difficult to control [36]. This lack of control causes the production of many other products which were generated during the polymerization process [37]. The chemistry of furans is very extensive, and many possible reactions can occur simultaneously with a heterogeneous system like the hydrothermal process.

Once the HTC process has finished, one of the fundamental steps for CNP production is the separation of the byproducts [38]. The hydrochar can be separated from the aqueous solution by simple filtration. Whereas, CNP is capable of being separated and classified by a number of different methods; such as: electrophoresis with polyacrylamide gel [39], dialysis [40], centrifugation [41] or solvents extraction [42]. In the solvent extraction method, the aqueous suspension is mixed with an organic solvent and the CNP migrate from the water to the solvent due to their chemical affinity. Solvents with different polarity can be used. It is important to mention that the amount of CNP removal will depend on the level of polarity.

This study aims to determine the effect that the organic solvent has on the production of CNP, under the condition of introducing a blend of water-organic solvent into the HTC reactor, considering that water is only used in a normal procedure. It is hypothesized that the CNPs that are formed during carbonization will cross from the water into the organic solvent inside the reactor and thus its mass yield can be improved keeping the properties of nanoparticles.

2. Materials and Methods

2.1. Chemicals:

D-(+)-Glucose, butyl acetate, hexane and toluene were obtained from commercial sources. Distilled water was used for all the experiments.

2.2. Synthesis:

2.2.1. Solvent extraction hydrothermal carbonization (SE): Dissolve 10 g of glucose in 300 mL of distilled water. The solution is placed in a stainless-steel reactor of 500 mL capacity. It is heated to 200 ^{o}C for a certain time (1, 2 or 4 hours), then the reactor is cooled down, and the hydrochar is separated by filtration, using a membrane filter of 0.45 um. The suspension is mixed with 100 mL of organic solvent (hexane, toluene or butyl acetate). The blend is let to settle for 10 minutes. Then, the phases are separated, and the organic phase is ultra-centrifuged for a time of 15 minutes at 20000 rpm. After that, the organic solvent is evaporated in a rotary evaporator, and finally the CNP are dried in a lab oven for two hours.

2.2.2. Solvent assisted hydrothermal carbonization (SA): Dissolve 10 g of glucose in 300 mL of distilled water, add 100 mL of organic solvent (hexane, toluene or butyl acetate) and place the blend into a stainless-steel reactor of 500 mL capacity. It is heated to 200 ^{o}C for a certain time (1, 2 or 4 hours), then the reactor is cooled down, and the hydrochar is separated by filtration, using a membrane filter of 0.45 um. The blend is settled for 10 minutes. Then, the phases are separated, and the organic phase is ultra-centrifuged for a time of 15 minutes at 20000 rpm. After that, the organic solvent is evaporated in a rotary evaporator, and finally the CNP are dried in a lab oven for two hours.

2.3. Characterization methods:

FESEM images were obtained by using a Carl Zeiss microscope. TEM images were taken using a TEM-200 microscope operating at 200 kV. Fourier transform infrared spectra of the materials in powder form were analyzed using a Perkin Elmer Spectrum Two FT-IR Spectrometer. The elemental analysis (C, H, and O) was performed using an ELEMENTAR VARIO CUBE Analyzer. Absorption spectra were made on Cary 60 UV-Vis Spectrophotometer. Emission spectra were measured with BioTek Synergy H1 spectrometer. Photoluminescence Quantum Yields were determined with an integrating sphere equipped on a Edimburgh Instruments FS5 spectrofluorimeter.

3. Results and Discussion

In this research, we evaluated the characteristics of the carbon nanoparticles obtained from two processes: solvent extraction hydrothermal carbonization (SE) and solvent assisted hydrothermal

carbonization (SA), the differences between the processes are explained above. In both processes, an organic solvent is used to separate the carbon nanoparticles from the liquid where they are dispersed. Three organic solvents were used for each process, each one with a different polarity (relative polarity: hexane 0.009, toluene 0.099, butyl acetate 0.241, water 1.000 [43]). The results of the mass yields of CNP are in table 1.

Table 1. Mass yields of carbon nanoparticles from SE-HTC and SA-HTC processes

	Mass Yield (%)					
Process / Time (h)	Solvent extraction (SE)			Solvent assisted (SA)		
	Hexane	Toluene	Acetate*	Hexane	Toluene	Acetate*
1	0.17	1.22	2.82	1.87	2.86	13.65
2	0.24	1.37	3.19	1.95	3.17	14.05
4	0.38	1.48	3.89	2.13	3.86	14.11

*Samples correspond to solvent: Butyl acetate

In the study carried out by Tang et al. [29] a solvent extraction method is performed to separate the quantum dots obtained from the hydrothermal carbonization of milk; three solvents were used: hexane, carbon tetrachloride and dichloromethane, obtaining mass yields of: 0.4%, 1.1% and 5.0% respectively. It is clearly observed that the amount of nanoparticles obtained increases when the polarity of the solvent is higher. This polarity effect is presented in the results of Table 1, in both processes: SE and SA, the mass yields of the CNP increases when an organic solvent with greater polarity is used, being butyl acetate the organic solvent with best results. In the case of hexane with the same solvent extraction process, there is a very similar mass yield (0.38%). However, the precursor is different. In the best of our knowledge, there is no investigation where the mass yields are obtained by using toluene, or butyl acetate, to have a reference point.

The type of process influences the mass yield, in table 1 it is observed that for the SA process the amounts of CNP obtained are much greater than those achieved with the SE process. This phenomenon occurs with all organic solvents and with all the reaction times. For example, with only one hour of reaction time, using the solvents: hexane, toluene and butyl acetate, the increase in the mass yields is: 1000 %, 134 % and 384 %, respectively. Consequently, introducing the organic solvent-water mixture into the reactor instead of just water improves incredibly the production of CNP. One possible reason for the formation of higher amount of CNP in the SA

process is described by Kuster [32], who mentions that HMF (Hidroximetilfurfural) can be hydrolyzed by taking two molecules of water from the medium to become levulinic acid and formic acid. Hence, if the HMF is not in the aqueous phase but it is actually in the organic one, its hydrolysis would be avoided and there would be a greater amount of HMF. In this case, during the SA process, the HMF would pass from the aqueous phase to the organic phase, hydrolysis would be prevented, and the aromatization and polymerization reactions would occur with a tendency to form CNP.

On the other hand, the reaction time does not influence considerably in the generation of CNP. For the two processes (SE and SA) at different reaction times, the percentage of mass performance remains almost constant. This is optimal to produce CNP due to the fact that within one hour of reaction, the same amount of CNP is practically obtained than with four hours of reaction. Besides, it reduces nanoparticles production cost because it involves a decrease in the energy that entails keeping the reactor to 200 ^{o}C. For this reason, from now, only the CNP obtained in the SE and SA processes with one hour of reaction are characterized.

Table 2. Elemental Analysis of CNP obtained in SE and SA processes with 1 hour of reaction time

Process	Sample code of CNP	C (wt%)	H (wt%)	O (wt%)	O/C*	H/C*
--	Glucose	40.00	6.67	53.33	1.00	2.00
SE	SE-Hexane	47.85	6.09	46.06	0.72	1.53
	SE-Toluene	54.13	6.90	38.97	0.54	1.53
	SE-Acetate	60.93	5.48	33.59	0.41	1.08
SA	SA-Hexane	52.71	6.52	40.77	0.58	1.48
	SA-Toluene	53.08	6.57	40.35	0.57	1.49
	SA-Acetate	65.14	4.89	29.97	0.35	0.90

*Atomic ratios

Table 2 shows the elemental analysis of the CNP obtained in all hydrothermal carbonization processes in 1 hour of reaction. Regardless of the type of process (SE or SA), the amount of C

increases, while the amount of O decreases, and in the case of H it remains mostly constant. In both processes, there is an influence of the organic solvent, when the polarity increases, higher carbon percentages are reached, and in some cases, up to 60% of C was reached, just like in the research carried out by Karak [28]. On the other hand, the percentage of oxygen decreases as the polarity of the solvent increases, which implies that the number of oxygenated groups decrease as the polarity index of the organic solvent is higher. With the percentages obtained, the atomic ratios; O/C and H/C were determined, these data are located in the Ven Krevelen diagram where the type of reaction that occurred in the HTC process can be observed (figure 1).

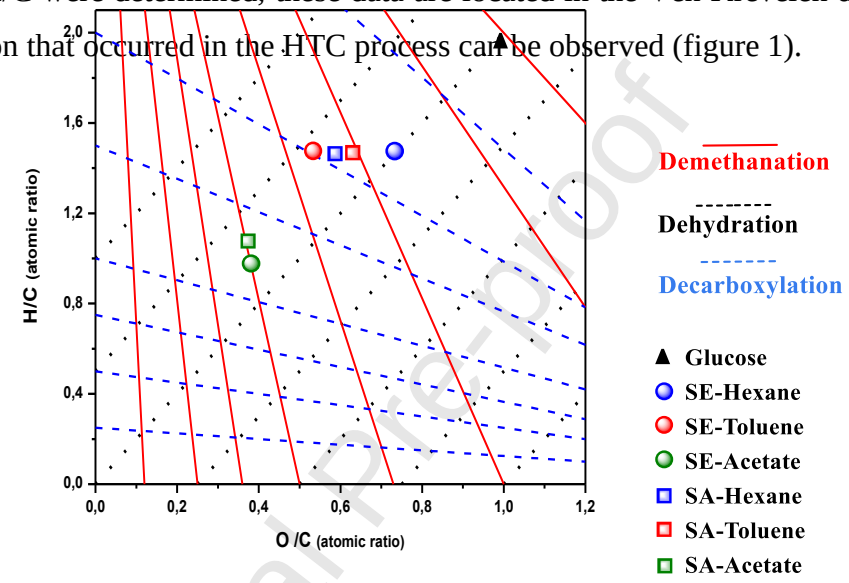

Figure 1. Venn Krevelen diagram for samples of the SE and SA processes with 1 hour of reaction time

Regardless the process being SE or SA, the reaction that governs the processes is dehydration, followed by decarboxylation, and for both processes demethanation does not take place. Compared with other solvents, butyl acetate reaches a greater dehydration; therefore, there is an effect of polarity on the degree of dehydration.

The changes in the chemical structures of the samples after the HTC process have been analyzed using FT-IR spectroscopy (figure 2) and compared with its precursor, glucose.

The band at 3370cm^{-1} corresponds to the O-H group (hydroxyl), the band at 2995cm^{-1} to C-H groups (aliphatic), while the band at 1650cm^{-1} is attributed to C=O (carbonyl and carboxyl) and

the 1395cm^{-1} band to C=C (aromatics), the band of 1046cm^{-1} is for C-O-C/ C-O groups (hydroxyl, ester, ether) and finally band 844cm^{-1} to C-H (aromatics).

In all the CNP of the SE and SA processes, the intensity of the bands corresponding to the hydroxyl group (3370cm^{-1}) is weaker than the glucose band. A decrease in the bands of the C-H groups (aliphatic) and an increase of the C=C and C-H (aromatics) bands is also observed. Considering that the O-H group is the functional group that banishes in dehydration and that the CNP are aromatic and non-linear systems, the results of the Ven Krevelen diagram confirm that the dehydration and aromatization take place during the HTC processes.

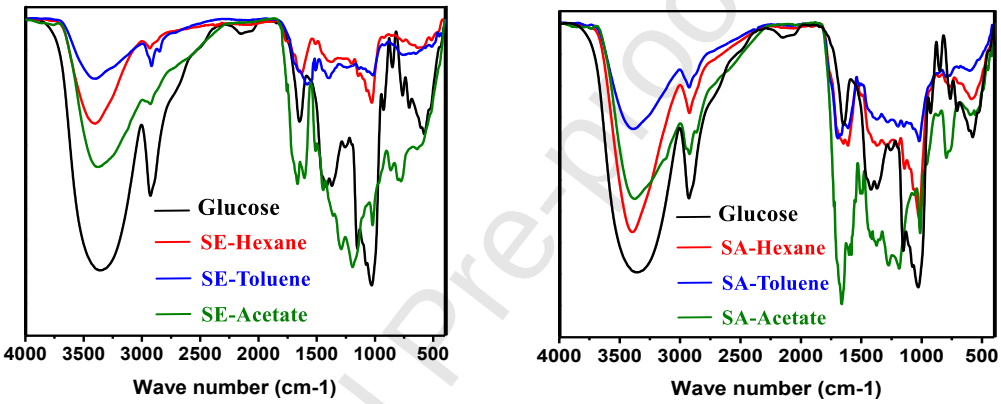

Figure 2. Infrared spectra for the CNP of SE and SA processes with 1 hour of reaction time

The carbonyl group (C=O) (one of the oxygenated groups that gives polarity to the CNP) has a different behavior; for the samples SE-Hexane and SE-Toluene the band decreases, while for samples SA-Hexane and SA-Toluene the band remains mostly constant. These four samples were made with hexane and toluene, which are the solvents with the lowest polarity. In contrast, for samples SE-Acetate and SA-Acetate, which were treated with the solvent with higher polarity, the intensity of the C=O band increases significantly, which happens to be the same for the bands of functional groups C-O-C/C-O. The latter is expected, since SE-Acetate and SA-Acetate samples have the highest amounts of C with regards to the other solvents, which can be seen in table 2. Similar analysis with the carbonyl band (C=O) was made by Wang et al. [44].

In the research conducted by Titirici et al. [35], the synthesis of carbon nanodots was made from glucose, similar to the procedure performed in this study. One of the conclusions from TEM images, is that the product of the reaction is a heterogeneous mixture of amorphous-like, carbon-

black type and various crystalline nanoparticles including carbon onions and expanded nanographite. Nevertheless, the research carried out by Tang et al. [45] also observed in the TEM images, a mixture of dispersed particles and amorphous CQD in the range of 2 to 6 nm. In this case, a similar result is recognized since the TEM and FESEM images (figure 3) indicate that there is a spherical CNP mixture with different sizes, along with amorphous carbonaceous material. In addition, very small amounts of CQD were observed. The ultra-centrifugation that is performed on the sample's treatment is fundamental for the process, because if it is not executed, a large amount of carbonaceous material is observed in the TEM and FESEM images, which prevents proper observation of the nanospheres. Although the TEM and FESEM used provide high resolution, the images are difficult to capture due to the low contrast that exists between the CNP and the carbon coated grids of the microscopes. Furthermore, when the electron beam of the equipment impinges on the nanoparticles, they become electrically charged and move or reflect light, which makes it challenging to obtain an image [35].

As mentioned above, one of the issues in the HTC is the high heterogeneity of the process, for that reason, the extraction with solvents (SE) permits the separation of the nanoparticles and their classification according to their chemical affinity. In the TEM and FESEM images of samples SE-Hexane and SE-Toluene, a small amount of nanospheres is observed in a matrix of amorphous carbonaceous material; but in sample SE-Acetate (figure 3) a high number of nanoparticles with diameters ranging from 34 nm to 122 nm is observed.

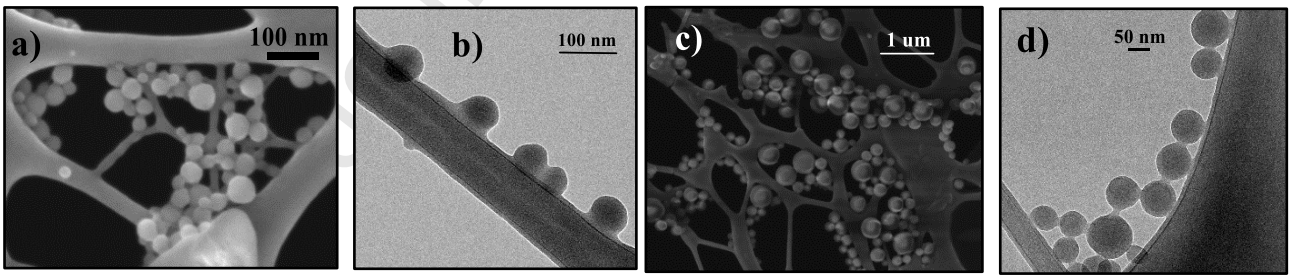

Figure 3. a) FESEM image for sample SE-Acetate, b) TEM image for sample SE-Acetate c) FESEM image for sample SA-Acetate, d) TEM image for sample SA-Acetate

In the SA process, a similar situation to the SE process occurs, for the SA-Hexane and SA-Toluene samples the TEM and FESEM images show small amounts of nanospheres in a matrix of amorphous carbonaceous material, while in the sample SA-Acetate, a great quantity of

nanospheres is observed (figure 3), with a size range of 80 nm to 275 nm. Both samples, SE-Acetate and SA-Acetate have a range of diameters highly dispersed; therefore, it can be stated that there is no relationship between the type of process and the size of the nanoparticles; thus, introducing a blend of organic solvent-water in the reactor doesn't assure a narrow size distribution of CNP.

One of the most important characteristics of the CNP is their optical properties. Figure 4a shows the absorption spectrum from all the samples of the hydrothermal carbonization processes. All spectra have a peak at 280 nm in the ultraviolet region with a tail that extends along the visible region. In addition to this, there is another peak at 327 nm with low intensity. According to the microscopy and FT-IR analysis, the samples are a mixture of nanospheres of different sizes and with different functional groups in their surface. However, each absorption spectrum is equal, which implies that the absorbance in the spectra is attributed to transitions π-π^* of the carbon double bonds (C=C) of the aromatic compounds that are in the carbon backbone of the nanospheres. There is hardly any influence of n-π^* transitions that produce C=O bonds that are on the surface of CNP. Hence, neither the size nor the functional groups on the nanoparticles surface influence the absorption spectrum.

Carbon nanospheres have a photoluminescence (PL) which depends on the excitation wavelength. Figure 4b shows the emission spectrum of the SA-Acetate sample at different excitation wavelengths, ranging from 300 nm to 480 nm. There are two fluorescence peaks, one at 345 nm corresponding to the blue color and the other with higher intensity at 495 nm corresponding to the green color. Blue PL and green PL are common in carbon nanoparticles [46,47]; regardless of the technique used for their synthesis.

All CNP, synthesized either by the solvent extraction method (SE) or by solvent assisted method (SA), have the same behavior in their emission spectrum, but they have different photoluminescence quantum yield (PL QY) which can be seen in table 3. Therefore, CNP emit light with the same wavelength, but with different intensity. Low quantum yields indicate that the recombination process of photogenerated electron-hole pair is non-radiative [48], possibly attributed to traps formed on the surface of the nanoparticles by an incomplete reaction [49]. However, the surface functional groups in the edge of CNP influence the rate of recombination of electron-hole pairs. The following is an explanation of this phenomenon. All synthesized CNP

have the same carbon backbone (polycyclic aromatic compounds), but the surface functional groups have different concentrations. The carbon backbone and the surface functional group, especially the C=O, cause the green PL in all CNP, but the concentration of surface functional groups make the recombination process of photogenerated electron-hole pairs be a radiative or non-radiative process.

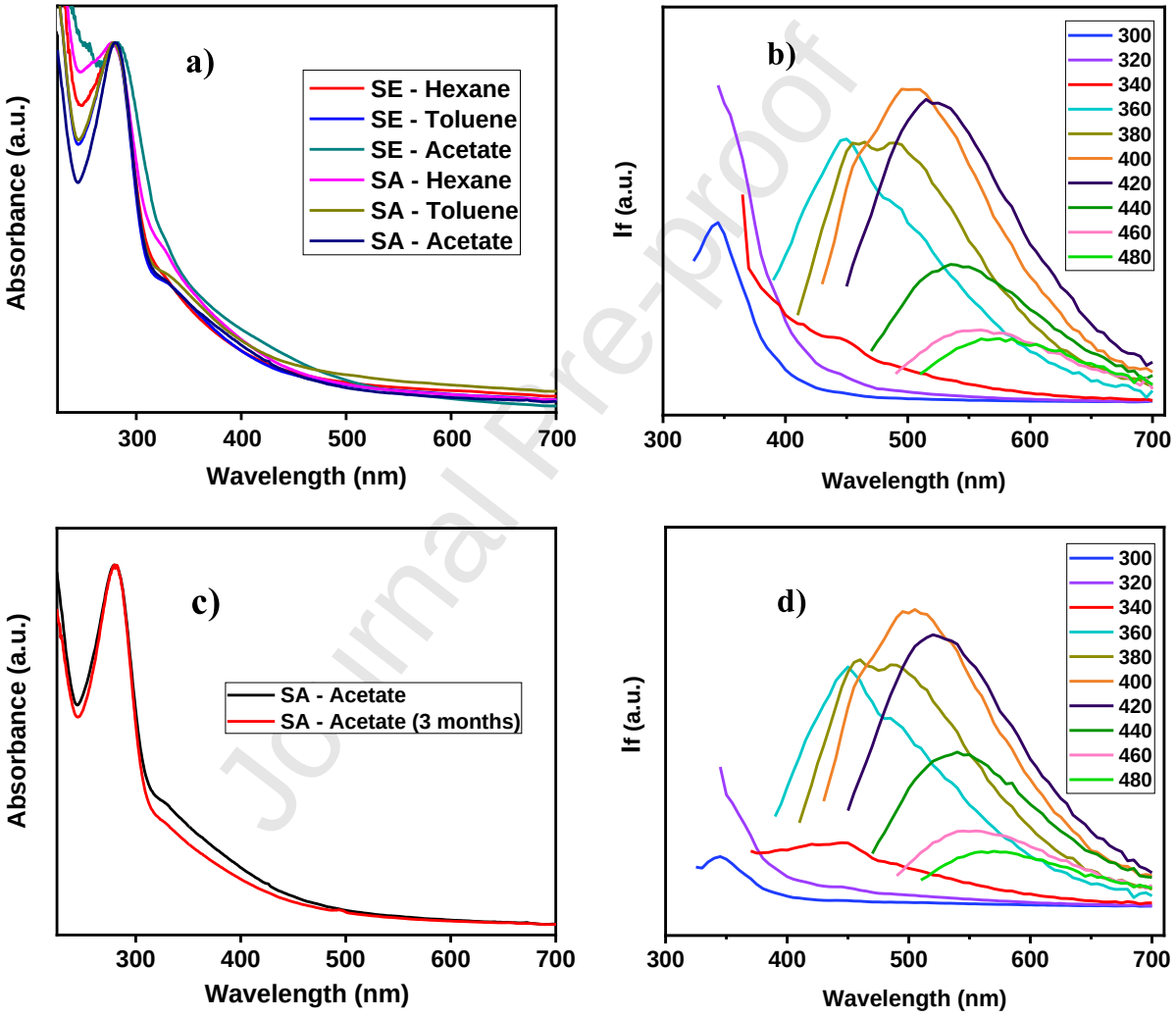

Figure 4. a) Absorption spectra for samples from SE and SA processes, b) PL spectra for sample SA-Acetate, c) Absorption spectra for sample SA-Acetate after three months of storage and d) PL spectra for sample SA-Acetate after three months of storage

In the study carried out by Wang et al. [44], PL QY depends on the quantity of carbonyl and carboxyl functional groups (C=O) in CNP. Higher intensity of the C=O band in FT-IR spectrum enhanced the PL QY. The samples SE-Acetate and SA-Acetate that have the highest intensity of absorption band of the carbonyl and carboxyl group (figure 2), are those that have a higher PL QY; 3.39% and 1.59% respectively. On the other hand, if we compare the synthesis process, all the CNP synthesized by the assisted solvent process (SA) have a lower PL QY than the samples synthesized by the solvent extraction process (SE). Wang et al. [44] in his study also mentions that this phenomenon is due to the fact that a higher intensity of the peaks in the region of 800 cm^{-1} to 1500 cm^{-1} in the FT-IR spectrum causes a decrease in PL QY.

Table 3. Photoluminescence Quantum Yield (PL QY) of CNP obtained in SE and SA processes with 1 hour of reaction time

Sample code of CNP	PL QY (%)
SE-Hexane	2.04
SE-Toluene	2.89
SE-Acetate	3.39
SA-Hexane	0.40
SA-Toluene	0.75
SA-Acetate	1.59

Since the SA-Acetate sample has the highest mass yield, it was stored for three months without protection from light. The absorption spectrum and the PL map from stored sample were achieved and compared with the non-stored sample. We can see in figures 4c and 4d, that not only the absorption and emission spectra are similar for both, but also new peaks are not found. Thus, we can say that the sample is photo-stable and doesn't lose its optical characteristics over time.

4. Conclusions

The amount of CNP that are generated in the HTC process depends on the kind of process utilized. SA process gives greater mass yields than the SE process. With only one hour of reaction

time, there is an increase in the mass yield of 1000 %, 134 % and 384 % for the solvents: hexane, toluene and butyl acetate respectively. Therefore, the introduction of a blend of organic solvent-water in the reactor instead of just using water enhances the production of CNP. In the SE and SA processes with butyl acetate; the highest degree of dehydration was achieved according to the Ven Krevelen diagram and the FT-IR spectra. In the case of the optical properties, the absorption and emission spectra are the same with both processes (SA and SE), for all the organic solvents. On the other hand, the Photoluminescence Quantum Yield depends of the kind of process and the organic solvent used, the best results are obtained with butyl acetate. Furthermore, CNP that had been stored for several months still maintain their optical properties.

Acknowledgment

This work has been carried out with the financial support of Universidad Central del Ecuador

References

[1] S. Ray, A. Saha, N. Jana, R. Sarkar, Fluorescent Carbon Nanoparticles: Synthesis, Characterization, and Bioimaging Application, Journal of Physical Chemistry C. 113 (2009) 18546 – 18551. https://doi.org/10.1021/jp905912n

[2] T. Lee, P.S. Alegaonkar, J.B. Yoo, Fabrication of dye sensitized solar cell using TiO2 coated carbon nanotubes, Thin Solid Films. 515 (2007) 5131 – 5135. https://doi.org/10.1016/j.tsf.2006.10.056

[3] Y. Guo, L. Zhang, S. Zhang, Y. Yang, X. Chen, M. Zhang, Fluorescent carbon nanoparticles for the fluorescent detection of metal ions, Biosensors and Bioelectronics. 63 (2015) 61 – 71. http://dx.doi.org/10.1016/j.bios.2014.07.018

[4] W.K. Oh, H. Yoon, J. Jang, Size control of magnetic carbon nanoparticles for drug delivery, Biomaterials. 31 (2010) 1342 – 1348. http://dx.doi.org/10.1016/j.biomaterials.2009.10.018

[5] B. Pan, B. Xing, Adsorption Mechanisms of Organic Chemicals on Carbon Nanotubes, Environmental Science and Technology. 42 (2008) 9005 – 9013. http://dx.doi.org/10.1021/es801777n

[6] M. Zhi, C. Xiang, J. Li, M. Li, N. Wu, Nanostructured carbon–metal oxide composite electrodes for supercapacitors: a review, Nanoscale. 5 (2013) 72 – 88. http://dx.doi.org/10.1039/c2nr32040a

[7] H. Li, X. He, Y. Liu, H. Huang, S. Lian, S.T. Lee, Z. Kang, One-step ultrasonic synthesis of

water-soluble carbon nanoparticles with excellent photoluminescent properties, Carbon. 49 (2011) 605 – 609. http://dx.doi.org/10.1016/j.carbon.2010.10.004

[8] Y. Fang, S. Guo, D. Li, C. Zhu, W. Ren, S. Dong, E. Wang, Easy Synthesis and Imaging Applications of Cross-Linked Green Fluorescent Hollow Carbon Nanoparticles, ACS Nano. 6 (2012) 400 – 409. https://doi.org/10.1021/nn2046373

[9] Q. Liang, W. Ma, Y. Shi, Z. Li, X. Yang, Easy synthesis of highly fluorescent carbon quantum dots from gelatin and their luminescent properties and applications, Carbon. 60 (2013) 421 – 428. http://dx.doi.org/10.1016/j.carbon.2013.04.055

[10] V. Singh, A. Mishra, Green and cost-effective fluorescent carbon nanoparticles for the selective and sensitive detection of iron (III) ions in aqueous solution: Mechanistic insights and cell line imaging studies, Sensors and Actuators, B: Chemical. 227 (2016) 467 – 474. http://dx.doi.org/10.1016/j.snb.2015.12.071

[11] J-H Liu, S-T Yang, X-X Chen, H. Wang, Fluorescent Carbon Dots and Nanodiamonds for Biological Imaging: Preparation, Application, Pharmacokinetics and Toxicity, Current Drug Metabolism. 13 (2012) 1046 – 1056. http://dx.doi.org/10.2174/138920012802850083

[12] O.Goryacheva, A. Novikova, D. Drozd, P. Pidenko, T. Ponomaryeva, A. Bakal, P. Mishra, N. Beloglazova, I. Goryacheva, Water-dispersed luminescent quantum dots for miRNA detection, TrAC - Trends in Analytical Chemistry. 111 (2019) 197 – 205. https://doi.org/10.1016/j.trac.2018.12.022

[13] S. Fiorito, A. Serafino, F. Andreola, A. Togna, G. Togna, Toxicity and Biocompatibility of Carbon Nanoparticles, Journal of Nanoscience and Nanotechnology. 6 (2016) 591 – l599. http://doi.org/10.1166/jnn.2006.125

[14] I. Kokalari, R. Gassino, A. Giovannozzi, L. Croin, E. Gazzano, E. Bergamaschi, A. Rossi, G. Perrone, C. Riganti, J. Ponti, I. Fenoglio, Pro- and anti-oxidant properties of near-infrared (NIR) light responsive carbon nanoparticles, Free Radical Biology and Medicine. 134 (2019) 165 – 176. https://doi.org/10.1016/j.freeradbiomed.2019.01.013

[15] M. Ajmal, U. Yunus, A. Matin, N. Ul Haq, Synthesis, characterization and in vitro evaluation of methotrexate conjugated fluorescent carbon nanoparticles as drug delivery system for human lung cancer targeting, Journal of Photochemistry and Photobiology B: Biology. 153 (2015) 111 – 120. https://doi.org/10.1016/j.jphotobiol.2015.09.006

[16] B. Selvi, D. Jagadeesan, B. Suma, G. Nagashankar, M. Arif, K. Balasubramanyam, M.

Eswaramoorthy, T. Kundu, Intrinsically Fluorescent Carbon Nanospheres as a Nuclear Targeting Vector: Delivery of Membrane-Impermeable Molecule to Modulate Gene Expression In Vivo, Nano Letters. 8 (2008) 3182 – 3188. https://doi.org/10.1021/nl801503m

[17] L. Cao, S. Sahu, P. Anilkumar, C.E. Bunker, J. Xu, K.A. Shiral, P. Wang, E.A. Guliants, K.N. Tackett, Y.P. Sun, Carbon Nanoparticles as Visible-Light Photocatalysts for Efficient CO2 Conversion and Beyond, Journal of the American Chemical Society. 133 (2011) 4754 – 4757. http://dx.doi.org/10.1021/ja200804h

[18] G.X. Chen, M.H. Hong, T.C. Chong, Preparation of carbon nanoparticles with strong optical limiting properties by laser ablation in water, Journal of Applied Physics. 95 (2004) 1455 – 1459. https://doi.org/10.1063/1.1637933

[19] V. Datsyuk, M. Kalyva, K. Papagelis, J. Parthenios, D. Tasis, A. Siokou, I. Kallitsis, C. Galiotis, Chemical oxidation of multiwalled carbon nanotubes, Carbon. 46 (2008) 833 – 840. https://doi.org/10.1016/j.carbon.2008.02.012

[20] J. Lu, J.X. Yang, J. Wang, A. Lim, S. Wang, K. Loh, One-Pot Synthesis of Fluorescent Carbon Nanoribbons, Nanoparticles, and Graphene by the Exfoliation of Graphite in Ionic Liquids, ACS nano. 3 (2009) 2367 – 2375. https://doi.org/10.1021/nn900546b

[21] A. Galvez, N. Herlin-Boime, C. Reynaud, C. Clinard, J. Rouzaud, Carbon nanoparticles from laser pyrolysis, Carbon. 40 (2002) 2775 – 2789. https://doi.org/10.1016/S0008-6223(02)00195-1

[22] S. Chandra, P. Das, S. Bag, D. Laha, P. Pramanik, Synthesis, functionalization and bioimaging applications of highly fluorescent carbon nanoparticles, Nanoscale. 3 (2011) 1533 – 1540. https://doi.org/10.1039/c0nr00735h

[23] M. Titirici, M. Antonietti, Chemistry and materials options of sustainable carbon materials made by hydrothermal carbonization, Chemical Society Reviews. 39 (2010) 103 – 116. https://doi.org/10.1039/b819318p

[24] M. Sevilla, A. Fuertes, Chemical and Structural Properties of Carbonaceous Products Obtained by Hydrothermal Carbonization of Saccharides, Chemistry - A European Journal. 15 (2009) 4195 – 4203. https://doi.org/10.1002/chem.200802097

[25] S. Chin, S. Yazid, S. Pang, S. Ng, Facile synthesis of fluorescent carbon nanodots from starch nanoparticles, Materials Letters. 85 (2012) 50 – 52. http://dx.doi.org/10.1016/j.matlet.2012.06.082

[26] M. Sevilla, A. Fuertes, The production of carbon materials by hydrothermal carbonization of cellulose, Carbon. 47 (2009) 2281 – 2289. http://dx.doi.org/10.1016/j.carbon.2009.04.026

[27] S. Sahu, B. Behera, T. Maiti, S. Mohapatra, Simple one-step synthesis of highly luminescent carbon dots from orange juice: application as excellent bio-imaging agents, Chemical Communications. 48 (2012) 8835 – 8837. http://dx.doi.org/10.1039/c2cc33796g

[28] B. De, N. Karak, A green and facile approach for the synthesis of water soluble fluorescent carbon dots from banana juice, RSC Advances. 3 (2013) 8286 – 8290. http://dx.doi.org/10.1039/c3ra00088e

[29] S. Han, H. Zhang, J. Zhang, Y. Xie, L. Liu, H. Wang, X. Li, W. Liu, Y. Tang, Fabrication, Gradient Extraction and Surface Polarity-Dependent Photoluminescence of Cow Milk-Derived Carbon Dots, RSC Advances. 4 (2014) 58084 – 58089. http://dx.doi.org/10.1039/c4ra09520k

[30] D. Sun, R. Ban, P.H. Zhang, G.H. Wu, J.R. Zhang, J.J. Zhu, Hair fiber as a precursor for synthesizing of sulfur- and nitrogen-co-doped carbon dots with tunable luminescence properties, Carbon, 64 (2013) 424 – 434. http://dx.doi.org/10.1016/j.carbon.2013.07.095

[31] H. van Dam, A. Kieboom, H. van Bekkum, The Conversion of Fructose and Glucose in Acidic Media: Formation of HydroxymethylfurfuraI, Starch - Stärke. 38 (1986) 95 – 101. https://doi.org/10.1002/star.19860380308

[32] B. Kuster, 5-Hydroxymethylfurfural (HMF). A Review Focussing on its Manufacture, Starch - Stärke. 42 (1990) 314 – 321. http://dx.doi.org/10.1002/star.19900420808

[33] S. Teong, G. Yi, Y. Zhang, Hydroxymethylfurfural production from bioresources: past, present and future, Green Chemistry. 16 (2014) 2015 – 2026. http://dx.doi.org/10.1039/c3gc42018c

[34] R. Li, A. Shahbazi, A Review of Hydrothermal Carbonization of Carbohydrates for Carbon Spheres Preparation, Trends in Renewable Energy. 1 (2015) 43 – 56. https://doi.org/10.17737/tre.2015.1.1.009

[35] N. Papaioannou, A. Marinovic, N. Yoshizawa, A. Goode, M. Fay, A. Khlobystov, M. Titirici, A. Sapelkin, Structure and solvents effects on the optical properties of sugar-derived carbon nanodots, Scientific Reports. 8 (2018) 1 – 10. http://dx.doi.org/10.1038/s41598-018-25012-8

[36] A. Funke, F. Ziegler, Hydrothermal carbonization of biomass: A summary and discussion of chemical mechanisms for process engineering, Biofuels, Bioproducts and Biorefining. 6 (2012)

246 – 256. https://doi.org/10.1002/bbb.198

[37] C. Falco, N. Baccileb, M.M. Titirici, Morphological and structural differences between glucose, cellulose and lignocellulosic biomass derived hydrothermal carbons, Green Chemistry. 13 (2011) 3273 – 3281. https://doi.org/10.1039/c1gc15742f

[38] Kokorina, A., Sapelkin, A., Sukhorukov, G., Goryacheva, I., 2019. Luminescent carbon nanoparticles separation and purification. Advances in Colloid and Interface Science. 274, 102043. https://doi.org/10.1016/j.cis.2019.102043

[39] M. Zarei, M. Zarei, M. Ghasemabadi, Nanoparticle improved separations: From capillary to slab gel electrophoresis, Trends in Analytical Chemistry. 86 (2017) 56 – 74. http://dx.doi.org/10.1016/j.trac.2016.11.004

[40] M. Xie, Y. Su, X. Lu, Y. Zhang, Z. Yang, Y. Zhang, Blue and green photoluminescence graphene quantum dots synthesized from carbon fibers, Materials Letters. 93 (2013) 161 – 164. http://dx.doi.org/10.1016/j.matlet.2012.11.029

[41] G. Oza, K. Oza, S. Pandey, S. Shinde, A. Mewada, M. Thakur, M. Sharon, M. Sharon, A Green Route Towards Highly Photoluminescent and Cytocompatible Carbon dot Synthesis and its Separation Using Sucrose Density Gradient Centrifugation, J Fluoresc, 25 (2015) 9 – 14. https://doi.org/10.1007/s10895-014-1477-x

[42] P. Zhao, L. Zhu, Dispersibility of carbon dots in aqueous and/or organic solvents, Chemical Communications. 54 (2018) 5401-5406. http://dx.doi.org/10.1039/C8CC02279H

[43] C. Reichardt, Solvents and Solvent Effects in Organic Chemistry, thrid ed.,Wiley-VCH, Weinheim, 2003

[44] L. Wang, S-J. Zhu, H-Y. Wang, S-N. Qu, Y-L. Zhang, J-H. Zhang, Q-D. Chen, H-L. Xu, W. Han, B. Yang, H-B. Sun, Common Origin of Green Luminescence in Carbon Nanodots and Graphene Quantum Dots, ACS Nano. 8 (2014) 2541 – 2547. https://doi.org/10.1021/nn500368m

[45] Z. Zhang, J. Hao, J. Zhang, B. Zhang, J. Tang, Protein as the source for synthesizing fluorescent carbon dots by a one-pot hydrothermal route, RSC Advances. 2 (2012) 8599 – 8601. http://dx.doi.org/10.1039/c2ra21217j

[46] S. Qu, X. Wang, Q. Lu, X. Liu, L. Wang, A Biocompatible Fluorescent Ink Based on Water-Soluble Luminescent Carbon Nanodots, Angewandte Chemie. 124 (2012) 12381 – 12384. http://dx.doi.org/10.1002/ange.201206791

[47] S. Zhu, Q. Meng, L. Wang, J. Zhang, Y. Song, H. Jin, K. Zhang, H. Sun, H. Wang, B. Yang,

Highly Photoluminescent Carbon Dots for Multicolor Patterning, Sensors, and Bioimaging, Angewandte Chemie - International Edition. 52 (2013) 3953 – 3957. http://dx.doi.org/10.1002/anie.201300519

[48] H. Wang, Z. Ye, C. Liu, J. Li, M. Zhou, Q. Guan, P. Lv, P. Huo, Y. Yan, Visible light driven Ag/Ag3PO4/AC photocatalyst with highly enhanced photodegradation of tetracycline antibiotics, Applied Surface Science. 353 (2015) 391 – 399. 353. http://dx.doi.org/10.1016/j.apsusc.2015.06.125

[49] Q. Wu, W. Li, J. Tan, Y. Wu, S. Liu, Hydrothermal carbonization of carboxymethylcellulose: One-pot preparation of conductive carbon microspheres and water-soluble fluorescent carbon nanodots, Chemical Engineering Journal. 266 (2015) 112 – 120. http://dx.doi.org/10.1016/j.cej.2014.12.089

AUTHOR STATEMENT

Diego Flores Oña: Formal analysis, Investigation, Resources, Data Curation, Writing - Original Draft, Visualization, Funding acquisition.

Andrés Fullana: Conceptualization, Methodology, Resources, Writing - Review & Editing, Supervision, Funding acquisition.

Declaration of interests

☒ The authors declare that they have no known competing financial interests or personal relationships that could have appeared to influence the work reported in this paper.

☒The authors declare the following financial interests/personal relationships which may be considered as potential competing interests:

Graphical abstract

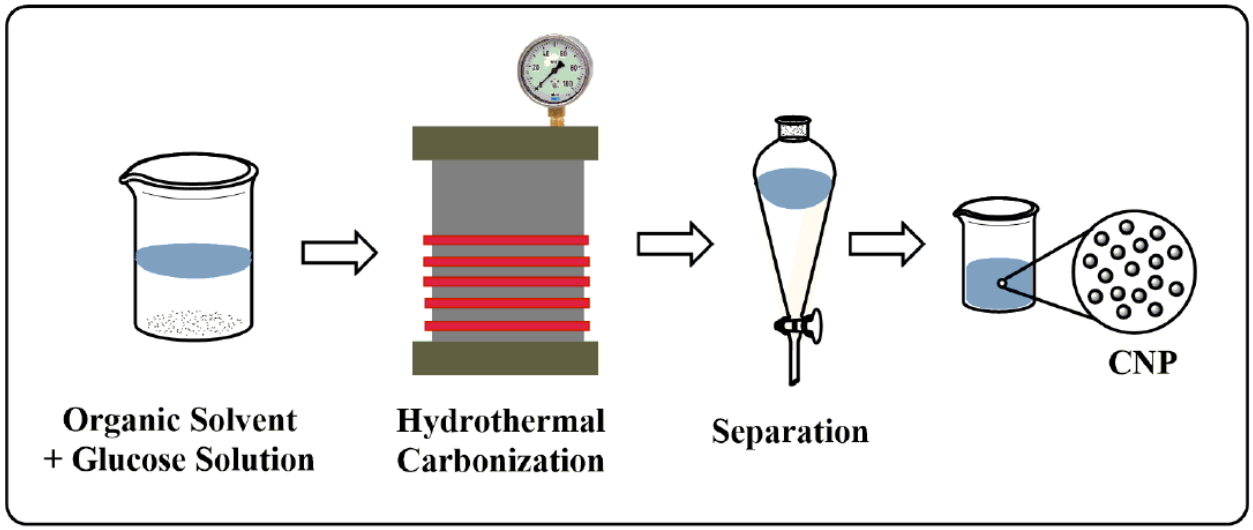

HIGHLIGHTS

- Synthesis method of carbon nanoparticles with high mass yields.
- Production of carbon nanoparticles with only one hour of reaction time.
- Carbon nanoparticles with good optical properties.